

Theoretical Study on the Aromaticity of the Pyramidal MB₆ (M = Be, Mg, Ca, and Sr) Clusters

Qian Shu Li* and Qiao Jin

School of Science, Beijing Institute of Technology, Beijing 100081, P. R. China

Received: April 17, 2003; In Final Form: July 22, 2003

A series of metal–polyboron clusters with the general formula MB₆ (M = Be, Mg, Ca, and Sr) were investigated using ab initio self-consistent field and density functional theory (DFT) methods. Calculation results show that the two clusters of BeB₆ and MgB₆ have C_{6v} pyramidal structure with M²⁺ cation interacting with a planar hexagonal B₆²⁻ dianion. Whereas the other two CaB₆ (C₁) and SrB₆ (C_s) clusters possess quasi-pyramidal structure with M²⁺ cation interacting with a chairlike B₆²⁻ dianion. Molecular orbital (MO) analysis and nucleus-independent chemical shifts (NICS) further reveal that the four MB₆ species all have three delocalized π MOs and two delocalized σ MOs and therefore exhibit the multiple-fold aromaticity.

1. Introduction

The concept of aromaticity originally developed from two-dimensional polygonal molecules often refers to cyclic, planar, or conjugated organic compounds with $4n + 2$ delocalized π electrons.^{1,2} In recent years this concept has been successfully extended from traditional organic molecules into pure all-metal clusters.^{3–10} Li and co-workers³ presented evidence of aromaticity for MAl₄⁻ (M = Li, Na, and Cu) purely metallic systems. The Al₄²⁻ dianion in a series of bimetallic clusters was found to possess two delocalized π electrons conforming to the $4n + 2$ electron counting rule for aromaticity. Similar aromaticity is found in Ga₄²⁻ and In₄²⁻ dianions⁴ in the gaseous NaGa₄⁻ and NaIn₄⁻ clusters due to the presence of two delocalized π electrons. Li et al.⁵ investigated the possibility of aromaticity in the heterocyclic four-membered ring XAl₃⁻ systems and found that the cyclic planar XAl₃⁻ (X = Si, Ge, Sn, and Pb) species have delocalized π electrons and therefore aromaticity. Aromaticity was also proposed in the 10 valence electrons B₃⁻, Al₃⁻, and Ga₃⁻ systems to explain the geometrical and electronic properties.⁶ The structural and electronic stability of the square-planar Hg₄⁶⁻ and Al₄²⁻ was attributed not only to π aromaticity due to the presence of the two π electrons, but also to σ aromaticity due to the occupation of the two four-center σ bonding orbitals.⁷ Zhan et al.⁹ first proposed the orbital analysis approach of the multiple-fold aromaticity for the square-planar Al₄²⁻ structure which can be determined by three independent delocalized (π and σ) bonding systems. Alexandrova et al.¹⁰ extended the σ aromaticity concept to small σ -aromatic alkali metal and alkaline metal clusters to explain relative stability of Li₃⁺ and Li₃⁻ ions.

Boron's remarkable abilities of forming three-center or multi-center bonds compensate for its electron deficiency. A lot of papers have been published on the pure boron clusters B_n.^{11–23} A few of the theoretical investigations in the literature have been reported on the metal–polyboron compounds.^{24–26} The best-known example of the metal–polyboron compounds is the structure of CaB₆ showed by Longuet-Higgins and Roberts²⁷ many years ago in which the two electrons are donated by the calcium atom to satisfy the bonding requirements of the boron octahedral. For rare-earth metal borides, LaB₆ is an emitter of

electron source, CeB₆ is known as a dense-Kondo material,²⁸ and SmB₆ is a so-called Kondo semiconductor with tiny energy gap.²⁹ In these solid-state metal borides, B₆ constitutes an octahedron B₆ cage and forms a three-dimensional network with metal atoms. However, the pyramidal metal borides have not been reported previously.

In the present paper, a series of the pyramidal MB₆ (M = Be, Mg, Ca, and Sr) species are theoretically investigated with ab initio and DFT methods. Molecular orbital (MO) analysis and the nucleus-independent chemical shifts (NICS)^{30–33} provide insight into the multiple-fold aromaticity of the pyramidal MB₆ clusters. The present study shows that the planar B₆²⁻ dianion (D_{2h}) with four π electrons is antiaromatic. Alexandrova et al.²² carried out the structure and bonding of B₆, B₆⁻, and B₆²⁻ and established the antiaromatic nature of chemical bonding for B₆⁻ and B₆²⁻. In addition, Ma et al.²³ also studied the dianionic B₆ cluster, and found the most stable B₆²⁻ (D_{2h}) having four π electrons is antiaromatic. Our results show that the pyramidal MB₆ (M = Be, Mg, Ca, and Sr) species have the multiple-fold aromaticity. It is an interesting thing that an antiaromatic B₆²⁻ dianion could be transformed into an aromatic one under the influence of the metal ions.

2. Computational Methods

All calculations were performed using the Gaussian 98 program package.³⁴ We initially optimized geometries and calculated frequencies of B₆²⁻, BeB₆, MgB₆, and CaB₆ species at the B3LYP/6-311+G* level of theory, where B3LYP is a DFT method using Becke's three parameter nonlocal exchange functional³⁵ with the nonlocal correlation of Lee, Yang, and Parr³⁶ and 6-311+G* is a split-valence triple- ζ plus polarization basis set augmented with diffuse functions.³⁷ We further studied B₆²⁻, BeB₆, MgB₆, and CaB₆ using the second-order Moller-plesset perturbation theory (MP2).³⁸ For the SrB₆ species, we optimized at the B3LYP and MP2 levels of theory, where the 6-311+G* basis set was used for boron and the LANL2DZ basis set was used for the heavier metal atom Sr (Z = 38). Minima were characterized with zero imaginary frequency and first-order saddle point with one imaginary frequency.

Molecular orbitals (MOs) for four MB₆ species were calculated by the HF method with the corresponding basis set. All MO pictures were made using the MOLDEN 3.4 program.³⁹

* Corresponding author. Fax: +86-10-68912665. E-mail: qqli@bit.edu.cn.

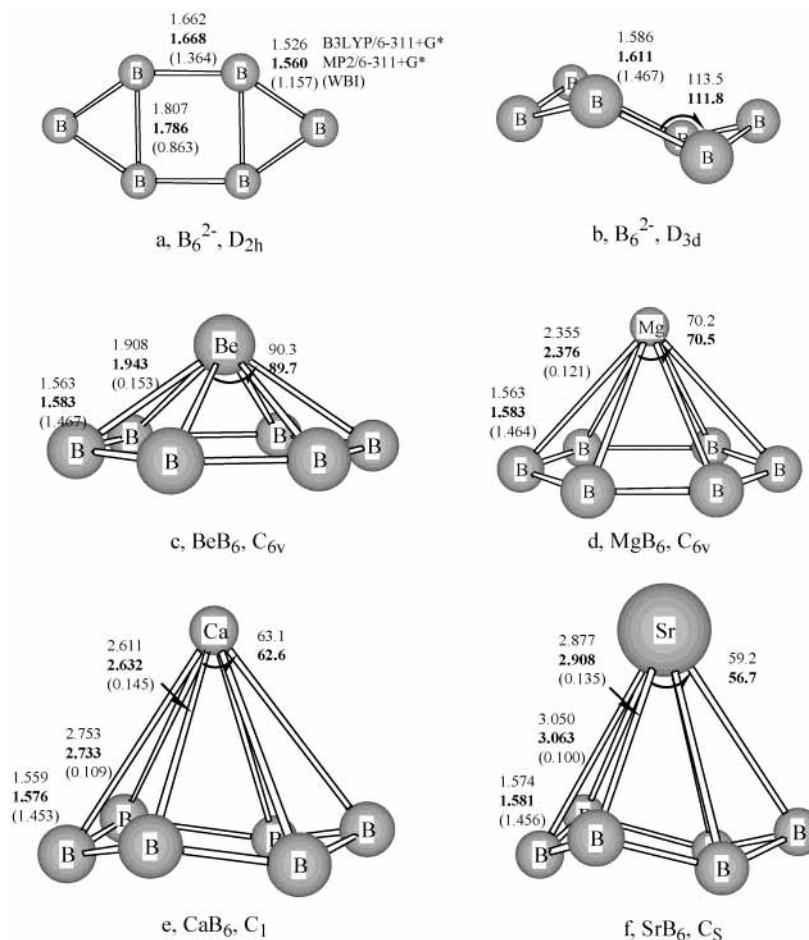


Figure 1. Optimized geometries (bond lengths in Å, bond angles in degrees) and the Wiberg bond indices (WBI) for BeB_6 , MgB_6 , CaB_6 , and SrB_6 species at the B3LYP and MP2 (bold font) methods.

TABLE 1: Total Energies (E),^a Zero-Point Energy (ZPE),^b and the Number of Imaginary Frequencies (NImag) for the BeB_6 , MgB_6 , CaB_6 , and SrB_6 Species^{c,d}

species	B3LYP			MP2		
	E	ZPE	NImag	E	ZPE	NImag
B_6^{2-} , (D_{6h})	-148.822932	12.72	0	-147.564183	12.36	0
B_6^{2-} , (D_{3d})	-148.696511	9.62	3	-147.562043	13.56	0
BeB_6 , (C_{6v})	-163.590033	15.89	0	-162.415881	15.49	0
MgB_6 , (C_{6v})	-348.905732	13.60	0	-347.350407	13.63	0
CaB_6 , (C_1)	-826.433001	13.01	0	-824.985832	13.45	0
SrB_6 , (C_s)	-179.234988	12.48	0	-178.388943	12.98	0

^a Total energies in Hartrees. ^b Zero-point energies in kcal/mol. ^c The 6-311+G* basis set was used for B, Be, Mg, and Ca, and the LANL2DZ basis set was used for the heavier metal Sr ($Z = 38$). ^d The listed total energies, ZPE, and NImag for CaB_6 are calculated at the MP2/6-31+G* level of theory.

NICS values for the four MB_6 species were calculated with the GIAO-HF/B3LYP method, where the 6-311+G* basis set was used for B, Be, Mg, and Ca, and the LANL2DZ basis set was used for Sr. The natural bond orbital (NBO)^{40–43} analysis was also performed to provide insight into the bonding nature and aromaticity of these species, and therein lies the explanation of the stability of the MB_6 species.

3. Results and Discussion

The optimized geometric structures and the Wiberg bond indices (WBI) for the four MB_6 species and B_6^{2-} dianion have been shown in Figure 1. Total energies, zero-point vibrational energies (ZPE), and number of imaginary frequencies of all species are summarized in Table 1. The vibrational frequencies of the BeB_6 , MgB_6 , CaB_6 , and SrB_6 species at the B3LYP and

MP2 methods are shown in Table 2. Calculated bond lengths (in Å), covalent radii of atom (in Å), and relative stability for BeB_6 , MgB_6 , CaB_6 , and SrB_6 species (B3LYP/6-311+G*) are listed in Table 3. The calculated NICS values are given in Table 4. MOs pictures for four MB_6 species are exhibited in Figure 2.

3.1. Geometric Structures and Vibrational Frequencies.

We performed ab initio and DFT methods on a wide variety of structures and found that all the ground-state pyramidal structures are local minimum with all real frequencies at the B3LYP and MP2 methods. Both BeB_6 and MgB_6 species have C_{6v} pyramidal structures with M^{2+} cations interacting with a planar hexagonal B_6^{2-} dianion. However, CaB_6 (C_1) and SrB_6 (C_s) possess quasi-pyramidal structures with M^{2+} cations interacting with a chairlike B_6^{2-} dianion.

TABLE 2: Calculated Vibrational Frequencies^{a,b} (in cm⁻¹) for the BeB₆, MgB₆, CaB₆, and SrB₆ Species

species	B3LYP						MP2					
	ω_1	ω_2	ω_3	ω_4	ω_5	ω_6	ω_1	ω_2	ω_3	ω_4	ω_5	ω_6
BeB ₆ , (C _{6v})	296	390	461	536	587	697	285	321	451	503	582	664
MgB ₆ , (C _{6v})	190	233	340	364	421	461	120	268	341	398	423	435
CaB ₆ , (C ₁)	156	224	273	318	353	414	255	262	269	339	366	389
SrB ₆ , (C _S)	170	245	252	258	358	474	221	241	255	295	339	397

^a The 6-311+G* basis set was used for B, Be, Mg, and Ca, and the LANL2DZ basis set was used for the heavier metal Sr. ^b Calculated vibrational frequencies for CaB₆ are calculated at the MP2/6-31+G* level of theory.

TABLE 3: Calculated Bond Lengths (in Å), Covalent Radii (in Å), and Zero-Point Corrected B3LYP Energies ΔE (in kcal/mol) for Hypothetical MB₆ → M + B₆ Reactions

	BeB ₆ , C _{6v}	MgB ₆ , C _{6v}	CaB ₆ , C ₁	SrB ₆ , C _S
B–B	1.563	1.563	1.559	1.574
M–B	1.908	2.355	2.611	2.877
sum of covalent radii of metal and boron	1.77	2.25	2.62	2.79
ΔE	68.2	1.5	29.5	5.6

TABLE 4: Calculated NICS Values (in ppm) with GIAO-HF/B3LYP Method for the BeB₆, MgB₆, CaB₆, and SrB₆ Species

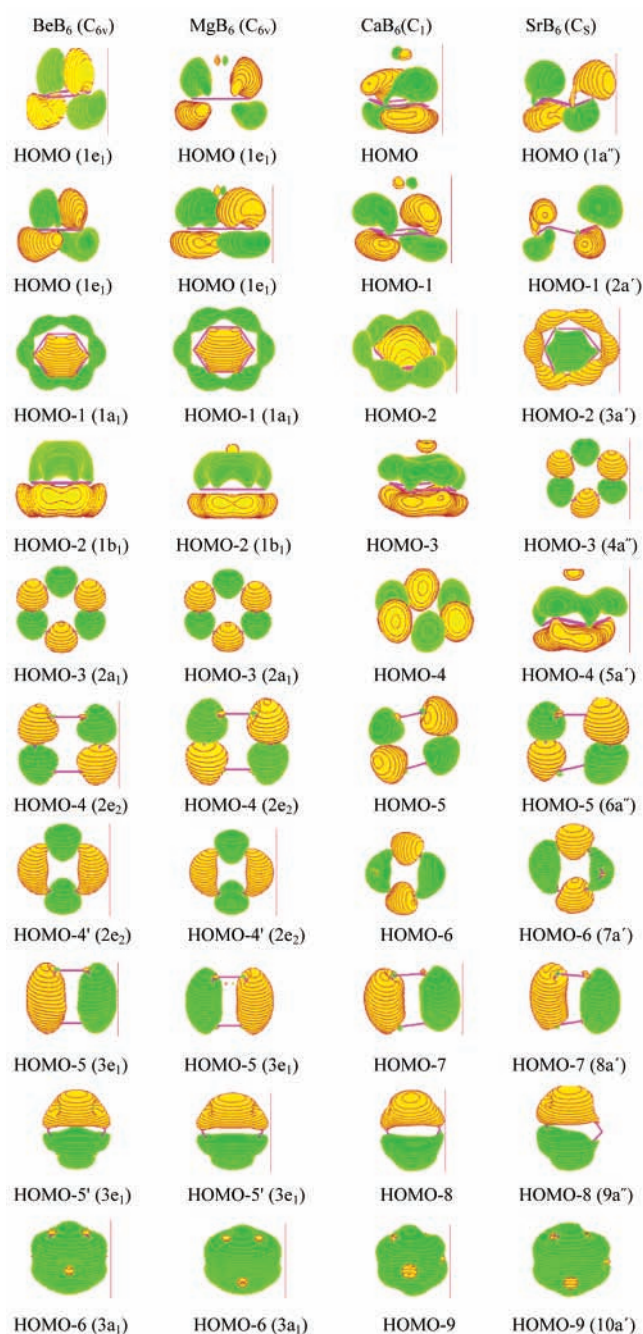
	BeB ₆	MgB ₆	CaB ₆	SrB ₆
NICS	-51.32	-44.27	-33.67	-29.56

^a Calculated NICS at the geometrical centers of the pyramidal structures.

Theoretical studies on various B₆²⁻ dianions showed that the planar hexagonal (*D*_{2h}) ring (Figure 1a) is the most stable dianion at the B3LYP/6-31+G*.^{22,23} The B–B bonds are not identical in the most stable *D*_{2h} planar structure. Chairlike *D*_{3d} structure (Figure 1b) is a third-order saddle point at the B3LYP/6-311+G* level of theory, while it is a local minima at the MP2/6-311+G* level of theory. There does exist a change in B–B bond distance in the MB₆ species and the B₆²⁻ dianion. For the pyramidal MB₆ species, all B–B distances are identical and slightly shorter than the average bond distance in the corresponding B₆²⁻ dianion (Figure 1a and b), and the extent of shortening shows a decreasing trend from Be to heavier metal atoms. This indicates that the lighter the metal atom is, the more important are the M²⁺ effects on the B₆²⁻ dianion.

As shown in Figure 1, the distances between metal atom and boron atom (1.908–2.877 Å) are much larger than those of the B–B (1.563–1.574 Å) in all the geometries of MB₆ species. Moreover, the larger the atomic number of the metal is, the longer the distance between metal and boron is and the smaller the angle of B–M–B is. The bond lengths of B–B in the four MB₆ species change slightly at the B3LYP and MP2 methods. The B–B bond lengths (1.563–1.574 Å) in the four MB₆ species are much shorter than the sum of covalent radii of two boron atoms (1.76 Å), indicating the existence of stronger B–B bonding. The M–B bond lengths in the four MB₆ species are longer than the sum of covalent radii of the corresponding metal atom and boron atom except for CaB₆. The covalent radii for the metal atoms and boron atom are 0.89, 1.37, 1.74, 1.91, and 0.88 Å for Be, Mg, Ca, Sr, and B, respectively.⁴⁴ In addition, the structures of CaB₆ and SrB₆ have chair conformation with identical B–B distances of 1.559 and 1.574 Å at the B3LYP method, respectively.

The calculated harmonic vibrational frequencies given in Table 2 show that the lowest frequencies of the BeB₆, MgB₆, CaB₆, and SrB₆ species are 296, 190, 156, and 170 cm⁻¹ at the B3LYP method and 285, 120, 255, and 221 cm⁻¹ at the MP2 method. The lowest vibrational frequencies calculated for the

**Figure 2.** Molecular orbital pictures of the BeB₆, MgB₆, CaB₆, and SrB₆ species, showing the HOMO down to the ninth valence molecular orbital.

four MB₆ species are larger enough to prove the minimum. The vibrational frequencies agree well at the B3LYP and MP2 methods for the four species (shown in Table 2).

3.2. Stability of the MB₆ Species. Natural population analysis indicates that alkaline earth metal atoms have positive charge

and boron atoms have negative charge in the four MB₆ species. The MB₆ species can be regarded as complexes of the B₆²⁻ dianion and metal M²⁺ cation. Bonding is due to electrostatic attraction effect between M²⁺ and B₆²⁻. The charges on the metal ions are Q(Be) = +1.49 e (BeB₆), Q(Mg) = +1.58 e (MgB₆), Q(Ca) = +1.61 e (CaB₆), and Q(Sr) = +1.65 e (SrB₆) (all are computed at the B3LYP/6-311+G*). NBO analysis shows that every WBI between metal and boron are 0.11–0.15, suggesting that M²⁺ cations have a role of stabilizing the B₆²⁻ dianion. The B₆²⁻ dianion might be stabilized in the form of a planar hexagonal (*D*_{6h}) ring by the interaction of its π system with Be and Mg atoms. However, the heavier alkaline earth metals cations Ca²⁺ and Sr²⁺ have effects on the electronic structure of the B₆²⁻ dianion. That induces changing of geometry of B₆²⁻ into the chairlike *D*_{3d} structure from the most stable planar (*D*_{2h}) ring structure. The calculated adjacent B–B WBI of the four MB₆ species is around 1.46, which is intermediate of the standard values of single-bond (1.0) and double-bond (2.0), indicating the existence of delocalization of electrons in the B₆²⁻ dianion.

The zero-point corrected B3LYP energies for hypothetical reactions MB₆ → M + B₆ are given in Table 3. The reaction is endothermic, indicating that the four MB₆ species are stable toward decomposition. The MB₆ species lie about 1.5–68.2 kcal/mol above the energy of a ground-state metal and the most stable B₆ (*C*_{2h}) cluster²³ at the B3LYP method. A simply energetic comparison of the MB₆ and B₆ cluster shows a substantial energy stabilization of the MB₆ species as compared to the bare B₆ cluster. On the basis of the above analysis, it is reasonably believed that the four MB₆ species have a quiet possibility of existence.

3.3. Aromaticity of the MB₆ Species. *3.3.1. Nucleus-Independent Chemical Shifts (NICS).* Aromaticity is often definable via magnetic criteria, such as NICS, which is based on the negative value of the magnetic shielding computed at or above the geometrical centers of rings or clusters. NICS is a simple and efficient aromaticity criterion in a wide range of molecules. Aromaticity is characterized by the negative NICS values (given in ppm), antiaromaticity is shown by positive NICS values, and nonaromatic compounds have NICS values close to zero.^{30–33} The more negative the NICS, the more aromatic the molecule is. In this study we calculated NICS values at the geometrical centers of the pyramidal structures for providing a direct measure of the ring current effects. NICS values of the BeB₆, MgB₆, CaB₆, and SrB₆ species at the GIAO-HF/B3LYP method are –51.3, –44.3, –41.5, and –29.6 ppm, respectively. NICS values for the four MB₆ species are all negative, suggesting the existence of delocalization and aromaticity in the four species. The antiaromaticity of the planar B₆²⁻ (*D*_{2h}) dianion with a positive NICS value above (by 1.0 Å) the geometric centers of the boron six-membered ring have been recently reported.²³ Here we have also calculated the NICS value of the planar B₆²⁻ (*D*_{2h}) dianion, which has a positive NICS value with the GIAO-B3LYP//B3LYP/6-311+G* level of theory above (by 1.0 Å) the geometric centers of the boron six-membered ring. Therefore, the plane B₆²⁻ (*D*_{2h}) dianion is antiaromaticity. When the metal ions are added to B₆²⁻ to form MB₆, the interaction of π system of B₆²⁻ dianion with the metal atoms occurs. This results in transformation of antiaromatic B₆²⁻ dianion into an aromatic one under the influence of the metal cations. We also found that NICS values for the four species increase with the increasing atomic number of the metal atom, indicating the decreasing of aromaticity of MB₆ species. For BeB₆ and MgB₆ species, the six boron atoms are locating in a

plane and easily forming cyclic π and σ electrons delocalization. Though the six boron atoms in CaB₆ species are not in a plane and have a chairlike structure, NICS value is –41.5 ppm at the GIAO-HF//B3LYP/6-311+G* level of theory and exhibit aromaticity due to the delocalization of π electrons and σ electrons.

3.3.2. Presence of 4n + 2 π Electrons and σ Electrons. In an orbital picture, three π delocalized MOs are first observed in the higher occupied molecular orbitals. As exhibited in Figure 2, the highest occupied molecular orbital (HOMO, 1e₁) of BeB₆ species includes two degenerated orbitals formed from the out-of-plane p orbitals. The two degenerate HOMO (1e₁) orbitals are delocalized π bonding MOs which render π aromaticity. The HOMO-1 (1a₁) and HOMO-3 (2a₁), formed from the in-plane p orbitals, are two six-center delocalized σ bonding orbitals that render σ aromaticity. The HOMO-2 (1b₁), formed from the out-of-plane p orbitals, is a delocalized π bonding orbital that renders π aromaticity. The two degenerated HOMO-4 (2e₂) MOs are linear combinations of s and p orbitals. The other three MOs are formed primarily from orbitals. In these occupied orbitals, HOMO (including two degenerated orbitals) and HOMO-2 are three delocalized π -bonding orbitals, containing six π electrons. HOMO-1 (1a₁) and HOMO-3 (2a₁) are σ delocalized MOs we would like to call σ -aromatic MO, each of the σ delocalized bonding systems containing two σ electrons. σ -Aromaticity initially introduced in hydrocarbons^{2,45,46} has been extended to metal, nonmetal, and metal–nonmetal clusters.^{7,9,10,23} The number of π electrons and σ electrons of BeB₆ species both satisfy the famous 4n + 2 electron counting rule and it is expected to have the multiple-fold aromaticity. The presence of delocalized π and σ orbitals have also played an important role in the stabilization of the metal–polyboron species. The MgB₆ species has a MO picture similar to that of the BeB₆ species.

For CaB₆ and SrB₆ species, the six boron atoms are not in a plane. The nonplanar B₆²⁻ diaion is greatly influenced by the heavier alkaline earth metal atoms. Even though CaB₆ and SrB₆ species with chairlike B₆²⁻ diaion have MOs similar to those of BeB₆ and MgB₆ except for the slight difference in ordering. But the MOs are distorted due to the presence of the heavier cations and showing the characteristic of chairlike B₆²⁻ structure. MO analysis shows that CaB₆ and SrB₆ species both have three π delocalized MOs and two σ delocalized MOs.

By comparing in Table 2 the MOs of B₆²⁻ reported in the literature²³ with the MOs of the four MB₆ species in this study, we found that the MOs of MB₆ and B₆²⁻ are different. For the *D*_{2h} B₆²⁻ diaion, the HOMO (B_{2g}) and HOMO-4 (B_{3u}) are π bonding MOs, containing four π electrons. It is seen to be a 4 π system conforming with the 4n electron counting rule and therefore antiaromatic.^{22,23,47} It is obvious that MB₆ has three occupied π MOs; two of them are the degenerated HOMO MOs, the other one is the HOMO-2 for BeB₆ and MgB₆, and HOMO-3 and HOMO-4 for CaB₆ and SrB₆, respectively. Thus, the four pyramidal MB₆ species are seen to be 6 π systems conforming with the 4n + 2 electron counting rule and therefore aromatic.

On the basis of the above MO analysis, π delocalized MOs and σ delocalized MOs contribute the property of the multiple-fold aromaticity for the four pyramidal MB₆ species, due to the presence of six π electrons and two σ electrons which follow the 4n + 2 electron counting rule. The delocalized π and σ MOs played an important role in stabilizing the four pyramidal BeB₆, MgB₆, CaB₆, and SrB₆ species.

4. Conclusion

We investigated a series of alkaline earth metal–polyboron clusters with the general formula MB₆ (M = Be, Mg, Ca, and

Sr) using ab initio and DFT methods, for which no report is found so far. Our calculation results showed that BeB₆ and MgB₆ possess C_{6v} pyramidal structures with a planar hexagonal B₆²⁻ dianion. Whereas CaB₆ (C₁) and SrB₆ (C_S) possess quasi-pyramidal structures with a chairlike B₆²⁻ dianion. From molecular orbital (MO) analysis and nucleus-independent chemical shifts (NICS) analysis, it is known that each of the four species has three delocalized π MOs and two independent delocalized σ MOs. Each of the delocalized chemical bonding systems satisfies the $4n + 2$ electron counting rule and therefore exhibits characteristic of the multiple-fold aromaticity.

References and Notes

- Garratt, P. *J. Aromaticity*; Wiley: New York, 1986.
- Minkin, V. I.; Glukhovtsev, M. N.; Simkin, B. Y. *Aromaticity and Antiaromaticity*; Wiley: New York, 1994.
- Li, X.; Kuznetsov, A. E.; Zhang, H. F.; Boldyrev, A. I.; Wang, L. S. *Science* **2001**, *291*, 859.
- Kuznetsov, A. E.; Boldyrev, A. I.; Li, X.; Wang, L. S. *J. Am. Chem. Soc.* **2001**, *123*, 8825.
- Li, X.; Zhang, H. F.; Wang, L. S.; Kuznetsov, A. E.; Cannon, N. A.; Boldyrev, A. I. *Angew. Chem., Int. Ed.* **2001**, *40*, 1867.
- Kuznetsov, A. E.; Boldyrev, A. I. *Struct. Chem.* **2002**, *13*, 141.
- Kuznetsov, A. E.; Corbett, J. D.; Wang, L. S.; Boldyrev, A. I. *Angew. Chem., Int. Ed.* **2001**, *40*, 3369.
- Boldyrev, A. I.; Kuznetsov, A. E. *Inorg. Chem.* **2002**, *41*, 532.
- Zhan, C. G.; Zheng, F.; Dixon, D. A. *J. Am. Chem. Soc.* **2002**, *124*, 14795.
- Alexandrova, A. N.; Boldyrev, A. I. *J. Phys. Chem. A* **2003**, *107*, 554.
- Berkowitz, J.; Chupka, W. A. *J. Chem. Phys.* **1964**, *40*, 2735.
- Hanley, L.; Whitten, J. L.; Anderson, S. L. *J. Phys. Chem.* **1988**, *92*, 5803.
- Bruna, P. J.; Wright, J. S. *J. Phys. Chem.* **1990**, *94*, 1774. Bruna, P. J.; Wright, J. S. *J. Mol. Struct.* **1990**, *210*, 243. Bruna, P. J.; Wright, J. S. *J. Chem. Phys.* **1989**, *91*, 1126. Bruna, P. J.; Wright, J. S. *J. Chem. Phys.* **1990**, *93*, 2617.
- Langhoff, S. R.; Bauschlicher, C. W. *J. Chem. Phys.* **1991**, *95*, 5882.
- Niu, J.; Rao, B. K.; Jena, P. *J. Chem. Phys.* **1997**, *107*, 132.
- Hernandez, R.; Simons, J. *J. Chem. Phys.* **1991**, *94*, 2961.
- Ray, A. K.; Howard, I. A.; Kanal, K. M. *Phys. Rev. B* **1992**, *45*, 14247.
- Kato, A. U.; Yamashita, K.; Morokuma, K. *Chem. Phys. Lett.* **1992**, *190*, 361.
- Kimura, K.; Takeda, M.; Fujimori, M.; Tamura, R.; Matsuda, H.; Schmechel, R.; Werheit, H. *J. Solid State Chem.* **1997**, *133*, 302.
- Boustani, I. *Surf. Sci.* **1996**, *370*, 355. Boustani, I. *Int. J. Quantum Chem.* **1994**, *52*, 1081. Boustani, I. *Chem. Phys. Lett.* **1995**, *233*, 273. Boustani, I. *Chem. Phys. Lett.* **1995**, *240*, 135.
- Li, Q. S.; Gu, F. L.; Tang, A. C. *Int. J. Quantum Chem.* **1994**, *50*, 173.
- Alexandrova, A. N.; Boldyrev, A. I.; Zhai, H. J.; Wang, L. S.; Steiner, E.; Fowler, P. W. *J. Phys. Chem. A* **2003**, *107*, 1359.
- Ma, J.; Li, Z. H.; Fan, K. N.; Zhou, M. F. *Chem. Phys. Lett.* **2003**, *372*, 708.
- Burdett, J. K.; Canadell, E.; Miller, G. J. *J. Am. Chem. Soc.* **1986**, *108*, 6561.
- Burdett, J. K.; Canadell, E. *Inorg. Chem.* **1988**, *27*, 4437.
- Thomas, P. F. *J. Solid State Chem.* **2000**, *154*, 110.
- Longuet-Higgins, H. C.; Roberts, M. de V. *Proc. R. Soc. London* **1954**, *A224*, 336.
- Komatsubara, T.; Sato, N.; Kunii, S.; Oguro, I.; Furukawa, Y.; Onuki, Y.; Kasuya, T. *J. Magn. Mater.* **1983**, *31–34*, 368.
- Kasuya, T.; Kasaya, M.; Takegahara, K.; Fujita, T.; Goto, T.; Tamaki, A.; Takigawa, M.; Yasuoka, H. *J. Magn. Mater.* **1983**, *31–34*, 447.
- Schleyer, P. v. R.; Maerker, C.; Dransfeld, A.; Jiao, H.; Hommes, N. J. v. E. *J. Am. Chem. Soc.* **1996**, *118*, 6317.
- Schleyer, P. v. R.; Jiao, H. *Pure Appl. Chem.* **1996**, *68*, 209.
- Schleyer, P. v. R.; Jiao, H.; Hommes, N. V. E.; Malkin V. G.; Malkina, O. L. *J. Am. Chem. Soc.* **1997**, *119*, 12669.
- Goldfuss, B.; Schleyer, P. v. R.; Hampel, F. *Organometallics* **1996**, *15*, 1755.
- Frisch, M. J.; Trucks, G. W.; Schlegel, H. B.; Scuseria, G. E.; Robb, M. A.; Cheeseman, J. R.; Zakrzewski, V. G.; Montgomery, J. A., Jr.; Stratmann, R. E.; Burant, J. C.; Dapprich, S.; Millam, J. M.; Daniels, A. D.; Kudin, K. N.; Strain, M. C.; Farkas, O.; Tomasi, J.; Barone, V.; Cossi, M.; Cammi, R.; Mennucci, B.; Pomelli, C.; Adamo, C.; Clifford, S.; Ochterski, J.; Petersson, G. A.; Ayala, P. Y.; Cui, Q.; Morokuma, K.; Malick, D. K.; Rabuck, A. D.; Raghavachari, K.; Foresman, J. B.; Cioslowski, J.; Ortiz, J. V.; Baboul, A. G.; Stefanov, B. B.; Liu, G.; Liashenko, A.; Piskorz, P.; Komaromi, I.; Gomperts, R.; Martin, R. L.; Fox, D. J.; Keith, T.; Al-Laham, M. A.; Peng, C. Y.; Nanayakkara, A.; Challacombe, M.; Gill, P. M. W.; Johnson, B.; Chen, W.; Wong, M. W.; Andres, J. L.; Gonzalez, C.; Head-Gordon, M.; Replogle, E. S.; Pople, J. A. *Gaussian 98*, Revision A.9; Gaussian, Inc.: Pittsburgh, PA, 1998.
- Becke, A. D. *J. Chem. Phys.* **1993**, *98*, 5648.
- Lee, C.; Yang, W.; Parr, R. G. *Phys. Rev. B* **1988**, *37*, 785.
- Hehre, W. J.; Radom, L.; Schleyer, P. v. R.; Pople, J. A. *Ab Initio Molecular Orbital Theory*; Wiley: New York, 1986.
- Møller, C.; Plesset, M. S. *Phys. Rev.* **1934**, *46*, 618.
- Schaftenaar, G. *MOLDEN 3.4*, CAOS/CAMM Center: The Netherlands, 1998.
- Carpenter, J. E.; Weinhold, F. *J. Mol. Struct. (THEOCHEM)* **1988**, *169*, 41.
- Foster, J. P.; Weinhold, F. *J. Am. Chem. Soc.* **1980**, *102*, 7211.
- Reed, A. E.; Curtiss, L. A.; Weinhold, F. *Chem. Rev.* **1988**, *88*, 899.
- Reed, A. E.; Weinstock, R. B.; Weinhold, F. *J. Chem. Phys.* **1985**, *83*, 735.
- Periodic Table of Elements*. Wiley-VCH: Weinheim, 1997.
- Cremer, D.; Binkley, J. S.; Pople, J. A.; Hehre, W. J. *J. Am. Chem. Soc.* **1974**, *96*, 6900.
- Chandraekhar, J.; Jemmis, E. D.; Schleyer, P. v. R. *Tetrahedron Lett.* **1979**, *39*, 3707.
- Havenith, R. W. A.; Fowler, P. W.; Steiner, E. *Chem. Eur. J.* **2002**, *8*, 1068.